Applied Catalysis B: Environmental 117–118 (2012) 1–9

Contents lists available at SciVerse ScienceDirect

Applied Catalysis B: Environmental

journal homepage: www.elsevier.com/locate/apcatb

Plasma assisted heterogeneous catalytic oxidation: HCCI Diesel engine investigations

Michael J. Kirkpatrick[a,*], Emmanuel Odic[a], Stéphane Zinola[b], Jacques Lavy[b]

[a] Department of Power and Energy Systems, E3S, SUPELEC, Gif-sur-Yvette, France
[b] IFP Energies Nouvelles, Rond-point de l'échangeur de Solaize, BP 3, 69360 Solaize, France

ARTICLE INFO

Article history:
Received 19 August 2011
Received in revised form 9 December 2011
Accepted 15 December 2011
Available online 10 January 2012

Keywords:
Diesel oxidation catalysis
Non-thermal plasma
Ozone
Unburned hydrocarbons
Carbon monoxide

ABSTRACT

A significant augmentation of the oxidation rate of carbon monoxide and unburned hydrocarbons has been previously demonstrated when the two processes of atmospheric pressure dielectric barrier discharge and Diesel oxidation catalysis were used simultaneously. In the case of carbon monoxide oxidation, the rate increase was attributed to a heterogeneous reaction of ozone with carbon monoxide. Ozone injection is investigated along with the direct application of the plasma to the gas upstream of a Diesel oxidation catalyst on a Diesel engine test bench. When used on the Diesel engine exhaust in steady state conditions, depending on the engine regime, the two processes had different effects on the gas composition. Both processes induced heating of the catalyst: while the plasma treatment of the entire gas flux heated the gas itself, and therefore also heated the catalyst, the injection of ozone heated the catalyst solely through the heat of reaction of ozone with the adsorbed species. Mechanisms for these effects are proposed and the performance of each approach is discussed in terms of energy cost and technical feasibility.

1. Introduction

Regulatory and market pressures continue to motivate the amelioration of technologies to reduce the emissions of motor vehicles [1]. Improvements can be made both through changes in combustion strategy and by improvements in the performance of the exhaust gas after-treatment system. Changes to the combustion strategy often involve the recirculation of engine exhaust gas into the cylinder (EGR), which causes lower combustion temperatures, leading to reduction in the production of nitrogen oxides [2]. Another technology, homogeneous charge compression ignition (HCCI), operates using the auto-ignition of a homogenous air–fuel–EGR mixture as opposed to timing based on spark ignition as in gasoline engines or fuel injection as in a standard Diesel engine. HCCI can lead to improvements in NO_x and particulate matter emissions while maintaining the high efficiency of conventional Diesel engines [3–6], but can also tend to lead to increases in emissions of unburned hydrocarbons and carbon monoxide. This study will consider after-treatment of and engine operated in HCCI mode with high EGR rates.

Because of changes in the proportions of emissions, research on EGR and HCCI technology must be coupled with progress on exhaust gas after-treatment systems specifically designed to handle more unburned fuel, carbon monoxide, and to some extent, more particulate matter. The use of non-thermal plasma in combination with catalysis has been considered for such applications [7–11], especially for intermittent use during cold start. In a recent publication [12], it was shown, at the laboratory scale (2–70 L/min) and in a cold start situation that the combination of plasma with simulated Diesel oxidation catalysis can result in improvements in catalyst performance. These improvements were shown to depend on both the treatment conditions (gas composition and temperature) and on whether the plasma treatment unit was placed directly in the exhaust gas line just upstream of the catalyst or used in parallel with the gas line to inject ozone just upstream of the catalyst. For the case of ozone injection, the reaction of ozone with carbon monoxide on the catalyst led to significant improvement of the catalyst performance for the oxidation of CO at low temperature. The heterogeneous reaction of CO with ozone has been reported on previously [10,13–15], and several patents have been obtained on the idea to inject ozone upstream of a catalyst for automotive applications [16–21]. Peterson et al. [15] found that the heterogeneous reaction of ozone with CO on platinum follows the Eley–Rideal mechanism, while the work by Roland et al. [10,13,14] found evidence that oxygen atom lifetime might be prolonged by interaction with the surface of typical catalyst washcoat materials such as alumina. The present work aims to investigate, using a full-scale vehicle Diesel engine running in steady-state conditions, the oxidation mechanisms induced by the combination of plasma

* Corresponding author.
E-mail addresses: mike.kirkpatrick@supelec.fr, mike.kirkpatrick@gmail.com (M.J. Kirkpatrick).

0926-3373/$ – see front matter © 2012 Elsevier B.V. All rights reserved.
doi:10.1016/j.apcatb.2011.12.022

with catalyst. From a process point of view, energy costs are considered but it should be highlighted that the objective was not make a full economic evaluation of the performance of an after-treatment device prototype, but simply to look at the feasibility of the combination of non-thermal plasma with catalysis on the Diesel engine scale.

2. Experimental

2.1. Plasma reactors, power supplies and electrical measurements

For the two different modes of operation (direct plasma treatment of the entire engine exhaust gas flux or ozone injection upstream of the catalyst), two different reactors were used. The reactor for the direct treatment was a parallel-plate design DBD reactor. Sixteen planar electrodes embedded in porcelain-type ceramic were separated by 0.7 mm gas gaps; the dimensions of the electrodes were 70 mm wide by 30 mm long, the length being measured along the axis of gas flow. In order to comply with the constraints corresponding to a real onboard power supply, a power converter was specifically designed (homemade at SUPELEC) to be connected to a 12.5 V source and to energize the primary winding of a high voltage transformer (transformation ratio: 420) whose secondary winding was then connected to the reactor. The high voltage signal had a frequency of 10 kHz and a peak-to-peak voltage ranging from 5 to 15 kV. The power delivered to the discharge reactor was constant at 355 W. A 71% overall energy conversion efficiency from the 12.5 V source to the discharge was measured.

The second reactor was a water-cooled ozonizer-type DBD reactor with coaxial cylinder geometry; a Pyrex tube (1.5 mm thickness, 75 mm external diameter with inner surface partially covered with a metallic layer connected to the power supply) was centered in a stainless steel tube (80 mm ID), giving a 2.5 mm gas gap. The active length of electrodes was 540 mm. This reactor was powered using a high voltage generator supplying a bidirectional high voltage signal (up to 31 kV peak-to-peak value) with a variable repetition rate (from 300 Hz to 8 kHz). Both the high voltage transformer and the power converter were homemade at SUPELEC and are described in more detail in an earlier publication [22]. Power delivered to the discharge reactor was 300 W, with an energy conversion efficiency of 81%.

For all experiments, electrical measurements were performed with a LeCroy 600 MHz – 10 GS/s Waverunner 62Xi oscilloscope. Voltage measurements were made using a Tektronix 75 MHz 1:1000 ratio P6015A high voltage probe and current measurements on the grounded side of the reactor (plasma DBD reactor or ozonizer-type DBD reactor) by measuring the voltage produced across two parallel 50 Ω BNC type low inductance resistors. These signals were used for discharge input measurements using the instantaneous current voltage product method. Power measurements were also verified using the Lissajous method when replacing the 50 Ω resistors by a 1 nF capacitor. The input power to the converters was also measured using conventional voltage and current probes in order to calculate the converter efficiency.

2.2. Catalyst

The catalyst used for the study was a conventional and commercially available Diesel oxidation catalyst (DOC) provided by Johnson Matthey, and is the same type that was used for the experiments in a previous study [12]. It was a cylindrical core cut out from a honeycomb structure cordierite monolith with a Al_2O_3 washcoat (including 10% in weight of hydrocarbon adsorbent material) and 100 g/ft^3 precious metal platinum/palladium in a 4/1 ratio. A 2.06 L monolith was used. For all experiments, the temperature was measured inside the catalyst core using a thermocouple probe which was placed about 1 cm from the inlet face of the catalyst where the maximum temperature is usually observed. Temperature measurements were also made by thermocouple just downstream of the catalyst. The catalyst cores were aged at Johnson Matthey using a standard method (800 °C for 24 h in 10 vol.% water).

2.3. Diesel engine and chemical measurements

The engine used was based on a Renault G9T, and adapted to run under HCCI conditions by some modifications (reduced compression ratio, narrow cone angle injectors with a dedicated piston chamber, reduced swirl number and highly cooled EGR system). The engine design, called narrow angle direct ignition (NADI^{TM}) [3–5], was able to run with HCCI combustion at low load and low speed. The exhaust gas was sampled both upstream and downstream of the post-treatment device (DOC alone, DBD plasma reactor + DOC, or ozone injection + DOC). Fig. 1 shows a photograph of the exhaust line with both the bypass line and the treatment line set up for the in-line treatment mode of operation. The exhaust gas flows from the engine outlet in the upper right of the image, through a selector valve and then through either the bypass or treatment line.

For catalyst testing, the exhaust line was fully instrumented with temperature sensors, pressure sensors and an O_2 sensor. The exhaust gases were analyzed by a Horiba 7100 DEGR system. This Horiba system comprised a paramagnetic oxygen analyzer, 2 FTIR CO_2 analyzers (1 for exhaust + 1 for EGR), a chemiluminescence-based NO_x analyzer, a FTIR CO analyzer, and a flame ionization detector (FID) for the measurement of hydrocarbons.

The fact that the engine was running in HCCI mode meant that the temperature ramp (catalyst light off) type experiments used in other work [12] were not possible, and had to be replaced by relatively 'steady state' tests. Two Diesel engine operating conditions were investigated, defined by motor speed and load (brake mean effective pressure – BMEP): 860 rpm – 0.2 bar BMEP (idle) and 1500 rpm – 2 bar BMEP. Whatever the engine running conditions, the exhaust gas pressure within the vicinity of the plasma remains close to atmospheric pressure. Steady state conditions in HCCI mode were first reached before the exhaust gas stream was diverted from a bypass line to the post-treatment system, which consisted of either the plasma device upstream of the DOC, or simply the DOC with a tube inserted upstream for ozone injection. For the steady state HCCI operation, the flow rate of exhaust gas emitted by the motor was either about 670 L/min or 900 L/min for the 860 rpm – 0.2 bar (idle) or 1500 rpm – 2 bar motor operating conditions, respectively; the corresponding space velocities in standard conditions (25 °C and 1,01,325 Pa) are 19,500 h^{-1} and 26,200 h^{-1}, respectively. The exhaust gas composition and operating conditions are given in Table 1.

3. Results

3.1. Direct plasma treatment of gas upstream of catalyst

For the direct treatment of the exhaust gas by the in-line plasma operation mode, the parallel-plate design DBD reactor was adapted to the motor exhaust line canning, and placed 55 mm upstream of the DOC. When turned on, 355 W were continuously dissipated in the discharge. Results for the motor running at idle are presented in Fig. 2. The periods during which the plasma was active are indicated by rectangles in the figure. The timing of the plasma on/off periods was chosen to allow for concentrations to stabilize and to characterize the experimental reproducibility. Three different temperature

Table 1
Summary of operating conditions.

Engine regime (speed – load)	860 rpm – 0.2 bar	1500 rpm – 2 bar
Inlet gas temperature (°C)	110	180–190
Catalyst core temperature (°C)	105–110	175
Total flow rate (L/min)	630–710	840–960
HCs (ppm[a])	960–1400	2700–2950
CO (ppm)	510–800	3900
NO_x (ppm)	32–36	5–10
CO_2 (%)	2.67	10.1
O_2 (%)	17.3	7.1
Energy density – plasma (J/L)	32	24
Energy density – ozone (J/L)	22	20

[a] C atom basis.

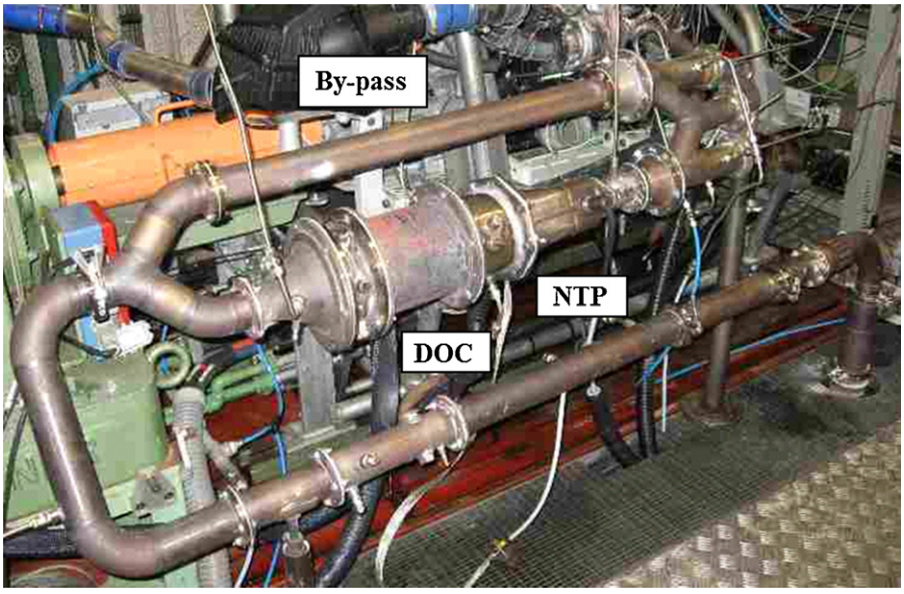

Fig. 1. Photograph of the in-line experimental setup. Exhaust gas flows from the engine at the upper right through a selector valve and then through either the bypass or the treatment line.

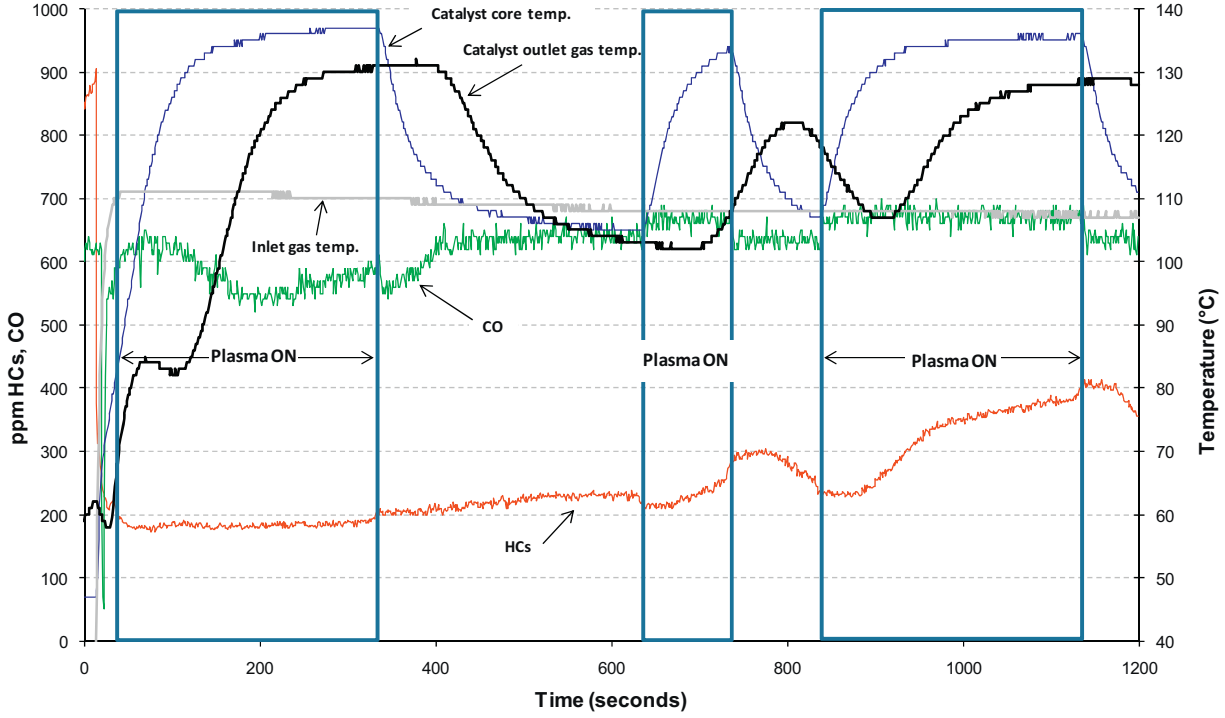

Fig. 2. Direct in-line plasma treatment of exhaust gas from engine running at 860 rpm, 0.2 bar; plasma treatment indicated by rectangles.

measurements are shown in the figure: first the temperature of the gas upstream of the plasma reactor (inlet gas temperature), then the temperature measured in the interior of the catalyst (catalyst core temperature), and finally the temperature measured by the thermocouple placed just downstream of the catalyst (catalyst outlet gas temperature). The first minute of experimental time during which the gas was diverted from the bypass line into the treatment system will not be commented on extensively, it can be noted however that the inlet gas temperature increased rapidly to about 110 °C, and then remained relatively stable. The catalyst core temperature clearly indicates the periods during which the plasma was turned on, which heated the gas by about 34 °C, and then decreased each time the plasma was turned off to a value lower to that of the inlet gas. The third temperature measurement downstream of the catalyst exhibited a delay of about 1 min with respect to the temperature measured inside the catalyst, and had about the same increase as was measured for the catalyst core when the plasma was turned on. The catalyst core temperature reached a maximum of about 135 °C and the downstream temperature about 130 °C; taking into account the delay, the downstream temperature was always inferior to that measured in the catalyst. A simple heat balance assuming that all the plasma power was converted into heat shows that a maximum temperature increase of about 36 °C could have been expected for this case. This can be considered very good agreement since some portion of the plasma power certainly goes toward heating the surrounding materials and not the gas. The heat balance was made using Eq. (1).

$$\Delta T = \frac{Q}{mC_p} \tag{1}$$

where Q represents the rate of heat transfer to the gas and m is the mass flow rate of the gas. Gas density was estimated based on the ideal gas law, using the measured pressure (always very close to atmospheric) and temperature. The value of the constant pressure heat capacity (data taken from the NIST standard reference database number 69) was estimated for each case based on a weighted average using the four major components of nitrogen, oxygen, water, and carbon dioxide. Table 2 provides a summary of the data used for the heat balance calculation.

As regards the effect of the plasma on the emissions measured downstream of the plasma – a quite limited effect is observed on hydrocarbons (HCs) (about 10 ppm removal estimated when the plasma is turned off at t = 330 s) along with a slight increase of the CO concentration (30 ppm), which comes from the partial oxidation of the removed HCs. An overall rise in the concentration of HCs is observed over the course of the entire experiment which is due to the dynamics of HC storage, and the fact that the HC adsorbent is becoming more and more saturated with HCs over the course of the experiment. The heat added by the plasma device causes a transient desorption of HCs, and then during the time between the application of plasma, the catalyst cools and a drop in the outlet HCs is observed due to a higher storage rate during this time. Therefore, the resulting observed level of HCs during the plasma operation in the outlet gas is a result of both HC removal from the bulk gas by the plasma and increased desorption from the catalyst caused by an increase in temperature. Despite the complexity of the variation of HC concentration due to the plasma heating effect on its storage and release by the adsorbent material in the catalyst, a 5% overall reduction of HC emissions when compared to the complete cycle without plasma was calculated by integration over the total experimental time.

Fig. 3 shows the results obtained at the 1500 rpm – 2 bar operating condition. The inlet gas temperature is significantly higher (about 175–185 °C) than at idle, as are the concentrations of CO and HCs. The temperature measured inside the catalyst again reflected the periods during which the plasma was turned on, however, the magnitude of the temperature increase observed to coincide with plasma operation was greater (40 °C) than for the idle condition (for the same plasma input power and higher gas flow rate – indicating another heat source). Unlike the case for the idle condition, a significant effect of the plasma on CO is observed for this case. The CO trend seems to quite closely follow the temperature measured just downstream of the catalyst and the decrease in CO concentration persists well after the plasma is turned off, suggesting that the effect is primarily thermal. The fact that the CO removal follows the downstream temperature more closely than the temperature measured inside the catalyst suggests that the downstream temperature might give a better description of the activation state of the catalyst. As for the HCs behavior, as had been observed for the idle condition, the fast effect of the plasma on HCs in the bulk gas is evident (even if modest) when the plasma is turned either on or off. Also similarly to the idle condition, the progression of the HC concentration shows that storage was important over the course of the experiment, and that the catalyst became more and more saturated with HCs during the first part of the experiment.

Unlike for the case of idle engine speed, for this case it can be shown that heterogeneous HC oxidation was taking place; the following argument for this assertion is based both on the thermal behavior of the system, and on the level of CO_2 emissions (Fig. 4). For this case the heat balance calculation, adjusting for the change in gas composition and flow rate, and with the same plasma input power, gave a temperature increase of only 27 °C compared to the observed 40 °C or more, a discrepancy which was not found for the idle condition. This discrepancy added to the fact that, contrary to the case for the idle condition, the catalyst outlet temperature is higher than the temperature measured inside the catalyst (reaching values exceeding 270 °C) leads to the conclusion that another heat source must be involved. The only other possible source of heat is that produced by exothermic catalytic reactions, i.e. the oxidation of HCs and/or CO.

In order to make an estimation of the temperature increase attributable to exothermic reactions, the amount of chemical throughput for a given reaction must be known. This is relatively straightforward for the case of CO, for example in Fig. 3, a change of CO concentration of about 900 ppm can be observed comparing the concentration at time t = 350 s and t = 600 s. The reaction which is occurring is presumably the oxidation of CO to CO_2, with a heat of reaction which can be calculated from the heats of formation of each species (obtained from the NIST standard reference database number 69):

$$CO + \frac{1}{2}O_2 \rightarrow CO_2 \quad -\Delta H = 283 \text{ kJ/mol} \tag{2}$$

For a reaction throughput of 900 ppm CO in a flow of 965 L/min (about 26 mol/min), a temperature change of the gas of about 8 °C was calculated. This 8 °C of temperature increase must be added to the 27 °C resulting from heat from the plasma as well as to the heating value from the reacting hydrocarbons in order to compare with the measured 40 °C or more gas temperature change. The calculation of heating due to reacting hydrocarbons was however complicated by two issues: uncertainty in the chemical throughput of this reaction pathway due to the dynamics of their adsorption and desorption on the catalyst, and uncertainty of the nature of the hydrocarbons themselves (only a measurement of total hydrocarbons in terms of carbon number was available). To deal with the uncertainty in the chemical throughput of hydrocarbons, the measurement of CO_2 was used to estimate the throughput indirectly. As shown in Fig. 4, for the same experimental times, the concentration of CO_2 changes by about 1200 ppm. While presumably about 900 ppm of this CO_2 comes from the oxidation of CO, the remainder must be due to the oxidation of HCs. As for the exact nature of the hydrocarbons being unknown, the heat of reaction

Table 2
Summary of values used in heat balance calculations – the gas densities used for the two cases were 860 rpm: $\rho = 0.91$ g/L; 1500 rpm: $\rho = 0.77$ g/L.

	F (L/min) (g/min)	C_p (J/g K)	Δppm CO	Δppm CO_2	ΔT (K) measured	ΔT (K) heat balance
860 rpm In-line	632 (575)	1.04	5	0	32–34	36
1500 rpm In-line	965 (745)	1.07	−900	1200	40	42
860 rpm Ozone	632 (575)	1.04	−120	420	7–12	13 (10)
1500 rpm Ozone	965 (745)	1.07	−280	500	10–12	12 (9)

was calculated for several different possible species: ethane, ethylene, propane, propylene, and iso-octane. The heat of reaction per mol of carbon was of course greatest for ethane and least for iso-octane, but the choice of the species did not have a huge effect on the total temperature change calculated by the heat balance: a variation of about ±6% was found depending on the choice of species. For the results presented here, the average of these 5 different species was used: −682 kJ/mol based on the number of moles of carbon. For a chemical throughput of 300 ppm of hydrocarbons, a temperature rise of just under 7 °C was estimated, giving a total of about 42 °C of temperature increase, corresponding well with the temperature change measured to occur within the catalyst. While it is not possible to explain the full magnitude of temperature increase measured downstream of the catalyst with these arguments, it is conceivable that some amount of HC oxidation took place which evolved heat, but that the CO_2 produced remained adsorbed on the catalyst, thereby masking the chemical evidence that it had taken place.

Again, in order to compare the overall performance of the system with and without plasma, if the HC concentration is integrated over the cycle and compared with a similar experiment without plasma as had been done for the idle condition, an overall reduction of 7% can be calculated. The two different cases may be interpreted as follows: at the idle condition, the exhaust gas is not hot enough to warm the catalyst up near to its light-off temperature, and so the additional heat added by the plasma has little effect on the catalyst activity, while in the bulk phase the plasma by itself converts a small quantity of HCs. At 1500 rpm – 2 bar, however, while the plasma also has a fast effect for this motor regime on the HCs concentration due to bulk phase reactions, the catalyst is already near its light-off temperature, and the plasma gives an extra thermal "push", which causes enough heterogeneous reaction throughput to start an autothermal reaction mechanism on the catalyst. This causes the reduction in CO concentration which had not been observed at the idle condition.

Comparing these results with those found on the synthetic gas bench scale [12], the reason that such different results were observed was that these tests were performed under steady state conditions (meaning the engine and exhaust line were already warmed up) whereas the synthetic gas bench scale tests simulated a cold start condition. At the elevated temperature, the production of ozone is reduced compared to either an in-line device during a cold start or an external ozone generator. Another difference is that the energy density of the plasma in this work (32 J/L and 24 J/L for idle and 1500 rpm – 2 bar, respectively) was less than that used on the bench scale. A higher energy density was not feasible in this work (because of overheating of the plasma device). Furthermore, it is unlikely that a higher energy density would have led to chemical as

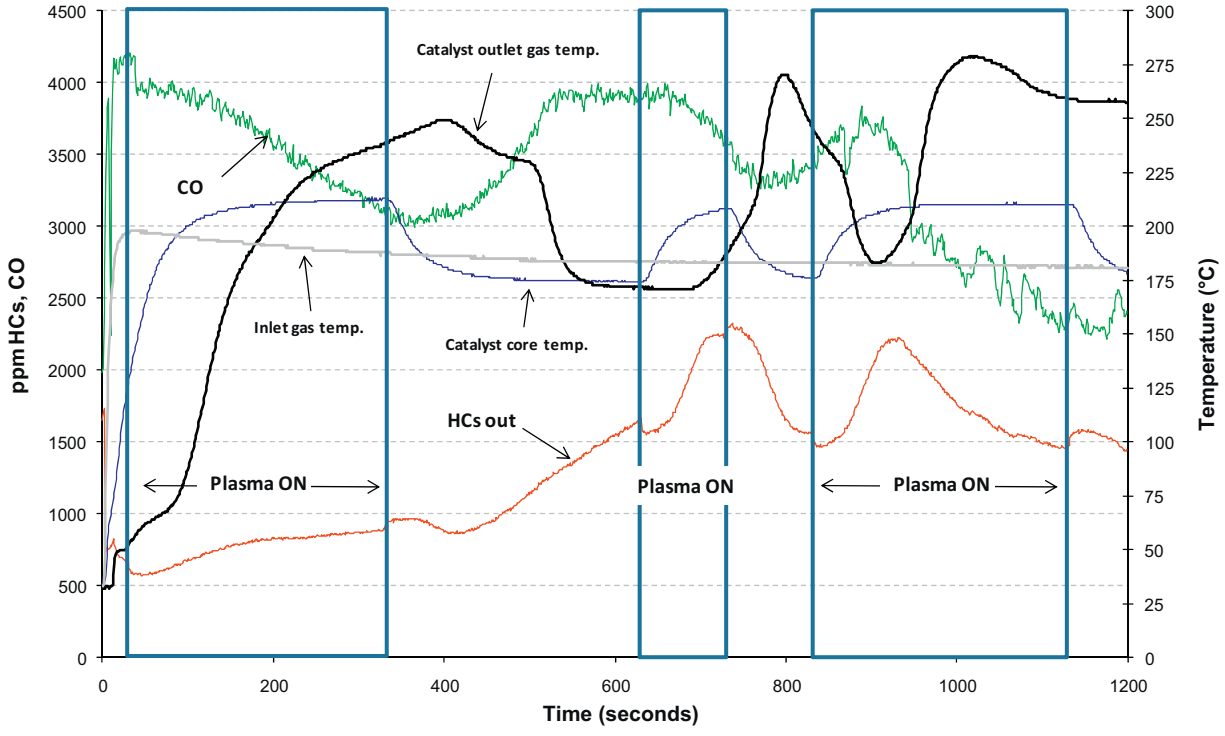

Fig. 3. Direct in-line plasma treatment of exhaust gas from engine running at 1500 rpm, 2 bar; plasma treatment indicated by rectangles.

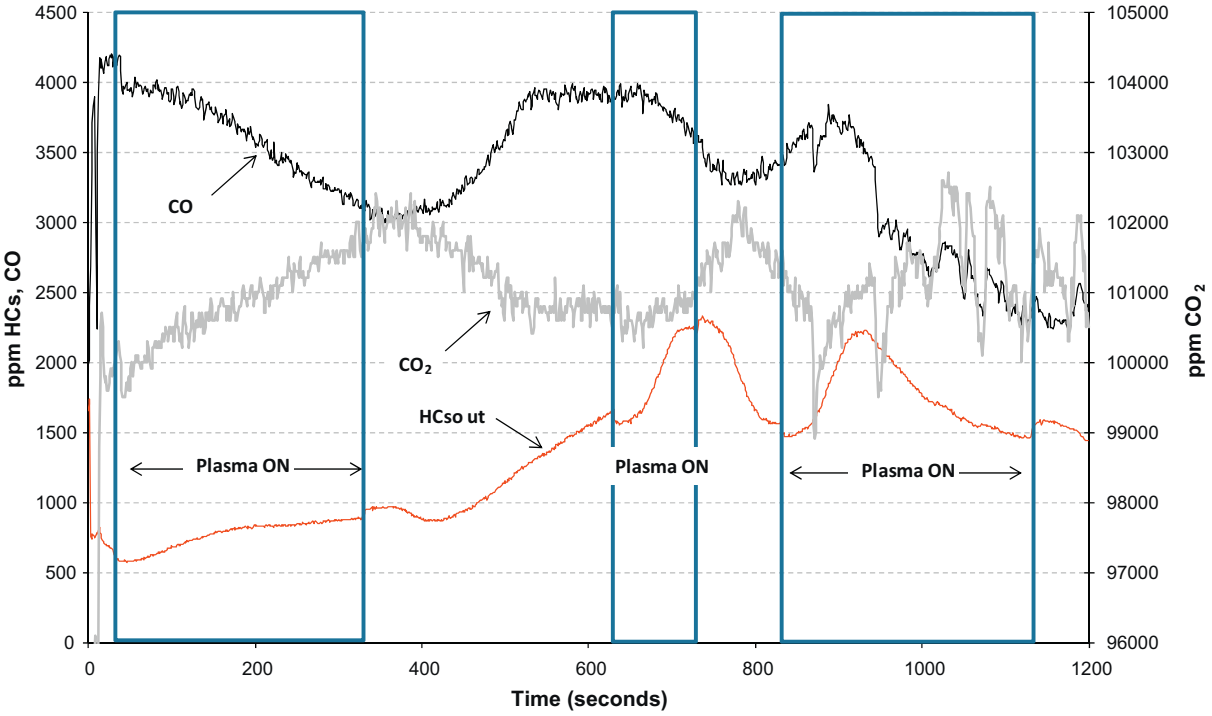

Fig. 4. Direct in-line plasma treatment of exhaust gas from engine running at 1500 rpm, 2 bar; plasma treatment indicated by rectangles. Same experiment as shown in Fig. 3 but with CO and CO_2 data.

opposed to thermal effects on the catalyst because the even higher resulting temperatures in the reactor would have further inhibited ozone production and further reduced excited species lifetime.

3.2. Ozone injection upstream of catalyst

Considering the effects previously observed on ozone injection upstream of the catalyst [12] and because the effect of the in-line treatment on the Diesel engine scale had been found to be largely thermal, ozone injection was also tested on the Diesel engine exhaust line. The ozone generator and its power supply (663 Hz, 10.5 kV peak, 300 W in discharge, 370 W consumed from the source) for this test, described in Section 2.1, were operated using a discharge power which gave an energy density (calculated using the total gas flow entering the catalyst, and not that in the ozone generator itself) which was in a same range as had been used for the in-line tests (26 J/L and 19.5 J/L for idle and 1500 rpm – 2 bar, respectively). Pure oxygen (20 L/min) was used to feed the ozone generator instead of air so as to have as large an amount of ozone injected as possible, seeing as the gas flow rate for the engine was much higher than the flow rate used in a previous study on a synthetic gas bench [12]. In a separate experiment using the same conditions, an ozone concentration of 12,800 ppm was measured for a flow rate of 20 L/min. For the two engine regimes, the injection of ozone would therefore result in approximately 370 ppm and 280 ppm for idle and 1500 rpm, respectively, assuming perfect mixing and neglecting any thermal degradation.

The gas flow containing ozone was injected into the center of the main gas flow using a capped tube which was perforated on one side (6 mm ID stainless steel, 8 mm OD) placed 200 mm upstream of the DOC. Two other positions for the injection were considered, one closer to the DOC (10 mm upstream of the DOC) and the other further upstream (400 mm upstream of the DOC). The close position resulted in inferior performance compared to the results to be presented here, likely due to the ozone not being spread across the entire inlet surface of the catalyst; the more remote injection location gave similar results to those found for 200 mm and so is redundant. Fig. 5 presents the results of an ozone injection experiment for the Diesel engine in HCCI mode at the idle operating point (860 rpm – 0.2 bar). The engine had been stabilized for several minutes to obtain relatively steady emissions before diverting the exhaust gas flow from the bypass line into the treatment line, turning on the oxygen flow and then activating the ozone generator. In the figure, the dilution caused by the addition of the flow of oxygen can be discerned at about 110 s experimental time, followed by the effect of ozone at 235 s. The ozone generator was turned on during two different time periods; first for a duration of 5 min followed by a shorter time of 2 min separated by an ozone off period of 2 min. During the periods of ozone injection, there was a significant effect on the concentration of CO, which was reduced by as much as 25%. The decrease in concentration of CO when the ozone generator was turned on was not as abrupt as its return to higher concentration when the ozone generator was turned off, which gives a clearer image of the contribution of ozone. The slow decrease in CO concentration upon the introduction of ozone contrasts with the observations made in previous work [12], where the initial decrease was very fast but then was followed by a slow rebound effect (the effect of the turning off of ozone was also fast in those experiments). The different results do not signify non-reproducibility because there were significant differences between the experiments. The most important difference was that the temperature of the catalyst for the steady state Diesel engine experiments (this work) was higher than for the bench scale experiments, which considered the performance of the process during a temperature ramp which began near ambient temperature. The largest effects of the plasma in that work were observed at low temperature. Another difference was that the speciation of hydrocarbons in this case was not controlled as was the case for the bench scale work, but it is not clear how this would affect the dynamics of the change in CO concentration, and so the temperature difference is the most likely explanation for the different observations between this work and that in the previous work. Storage on the catalyst again played a

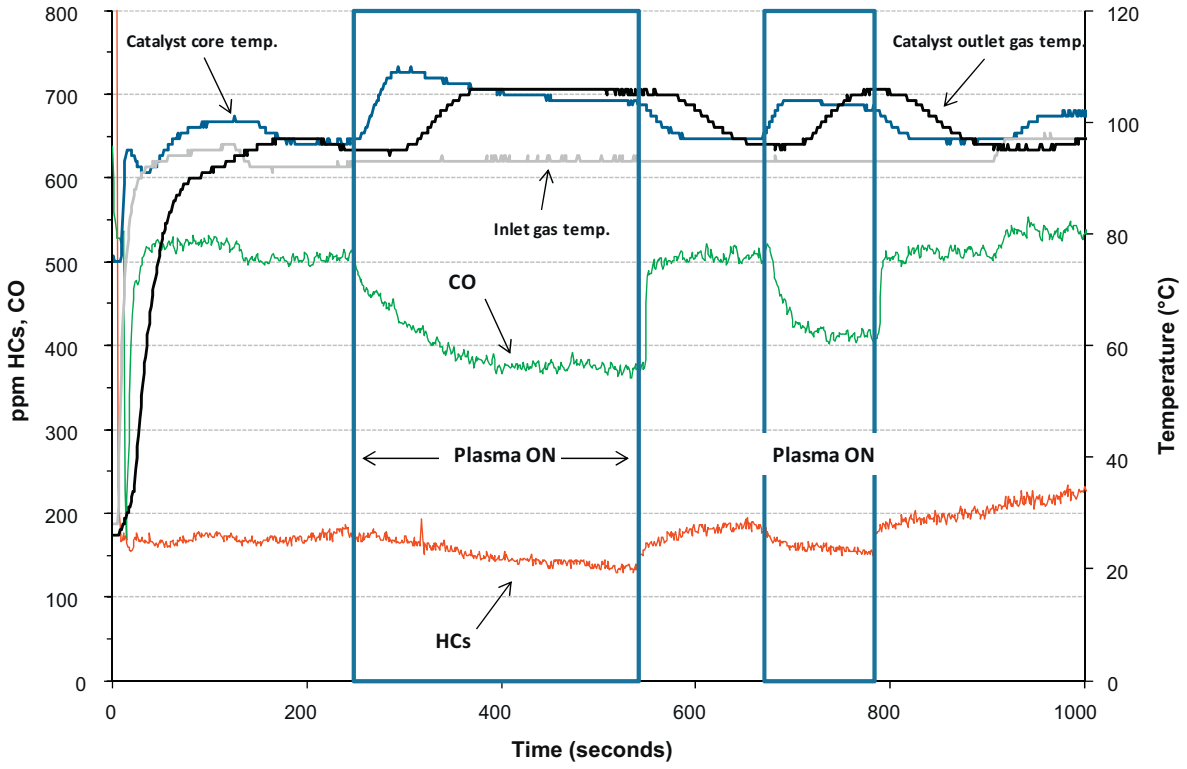

Fig. 5. Ozone injection experiment on exhaust from engine running at 860 rpm, 0.2 bar. Ozone injection indicated by rectangles.

role in the dynamics of the measured hydrocarbon concentration in the outlet gas, nevertheless, an effect of the injection of ozone on the hydrocarbon concentration is observed, especially when the ozone generator was turned off. Fig. 6 shows some of the same data as Fig. 5, but with the CO_2 data added, and a sharp decrease in CO_2 concentration corresponding to the sharp increase in CO can be seen at the moments when the ozone generator is turned off.

The same three different temperature measurements which were reported for the inline experiments are again shown in Fig. 5 – however, in this case, any temperature rise is only attributable to exothermic reactions because the ozone generator was cooled and additionally, was separated from the ozone injection point by about three meters of Teflon tube, which brought the ozone/oxygen gas flow very near to ambient temperature before entering the exhaust line. The temperature measurements indicate an increase in temperature of between 7 °C and 12 °C. Again, a heat balance was made much as discussed for the inline case, but this time considering only exothermic reactions to explain the rise

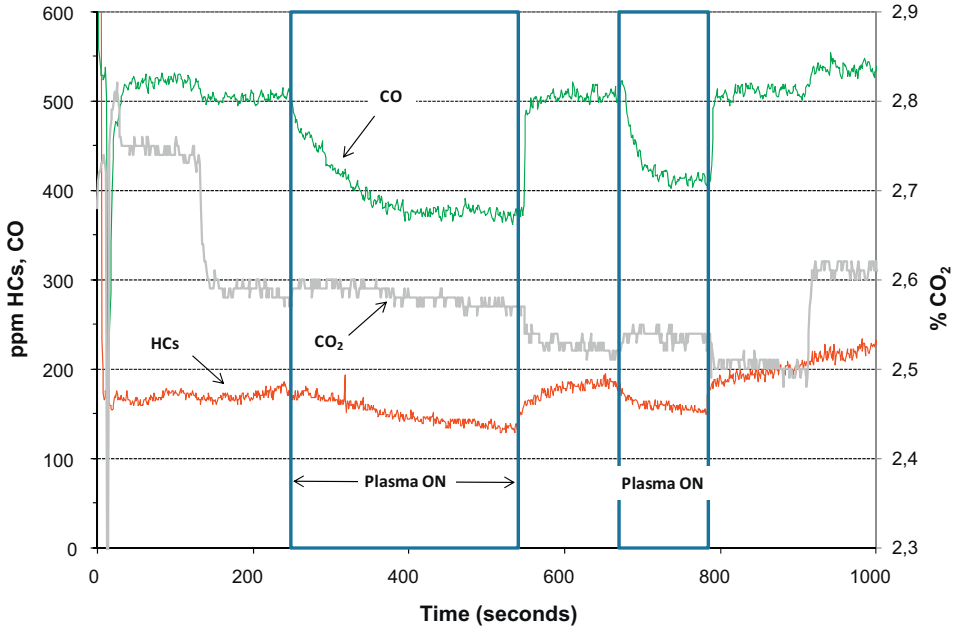

Fig. 6. Ozone injection experiment on exhaust from engine running at 860 rpm, 0.2 bar. Ozone injection indicated by rectangles. Same experiment as shown in Fig. 5 but with CO and CO_2 data.

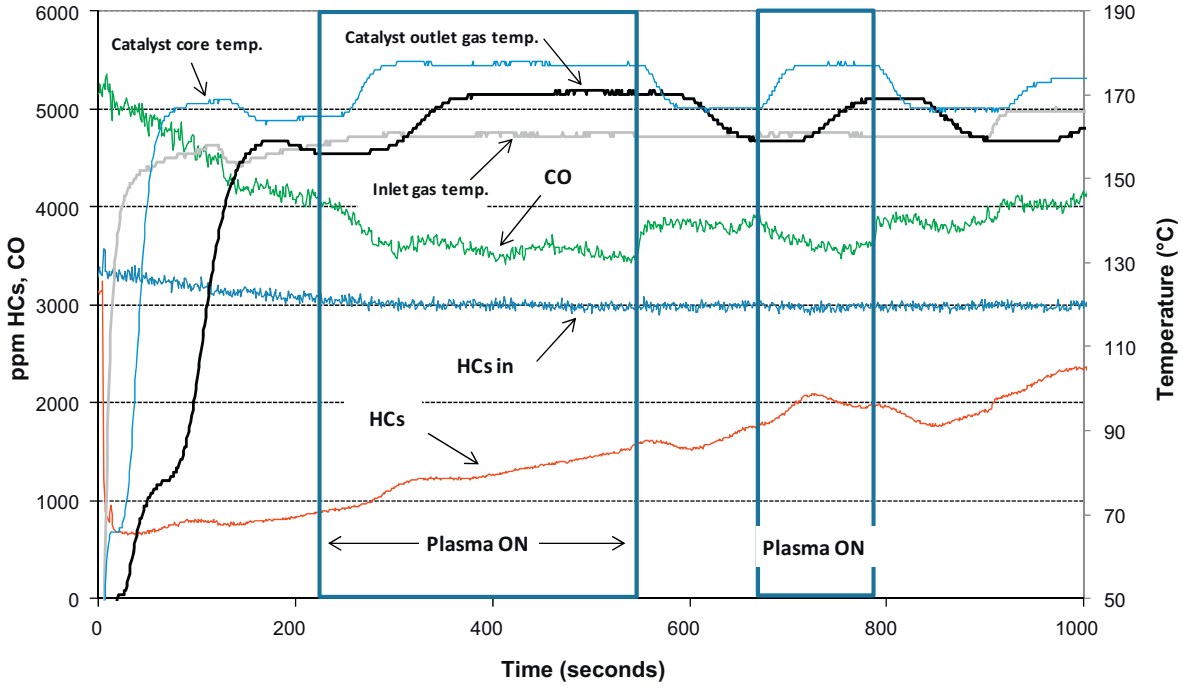

Fig. 7. Ozone injection experiment on exhaust from engine running at 1500 rpm, 2 bar. Ozone injection indicated by rectangles.

in temperature. Some uncertainty lies in the exact stoichiometry of the ozone reactions. For example, the assumption can be made that the reactions follow the type outlined by Peterson et al.; i.e. the reaction of ozone with carbon monoxide follows the stoichiometry given by Eq. (3):

$$CO + O_3 \rightarrow CO_2 + O_2 \quad -\Delta H = 426\,\text{kJ/mol} \tag{3}$$

Depending on the stoichiometry used for the reaction of ozone with carbon monoxide and unburned hydrocarbons, the heat balance calculation indicates that a temperature increase of between 10 °C and 13 °C might be expected based on the chemical throughput and gas flow conditions. The upper bound of 13 °C for the temperature increase calculation corresponds to the assumption of stoichiometry like that of reaction (3). However, there is a problem with the assumption that the entire reaction throughput observed in the experiments proceeded in this fashion. According to measurements made before the Diesel engine test bench experiments, only about 370 ppm of ozone should have been produced while a change in outlet CO_2 concentration of about 420 ppm was observed (this discrepancy was even more pronounced for the case of 1500 rpm engine operating regime, where the numbers were 280 ppm O_3 vs 500 ppm CO_2). This means that one mole of ozone led to more than one mole of reaction throughput based on carbon. The precise stoichiometry which occurred in these experiments is difficult to determine based on the available evidence, and would be interesting for further investigation with online ozone measurements. What can be stated is that the observed temperature increase is in agreement (with a margin of error that comprises

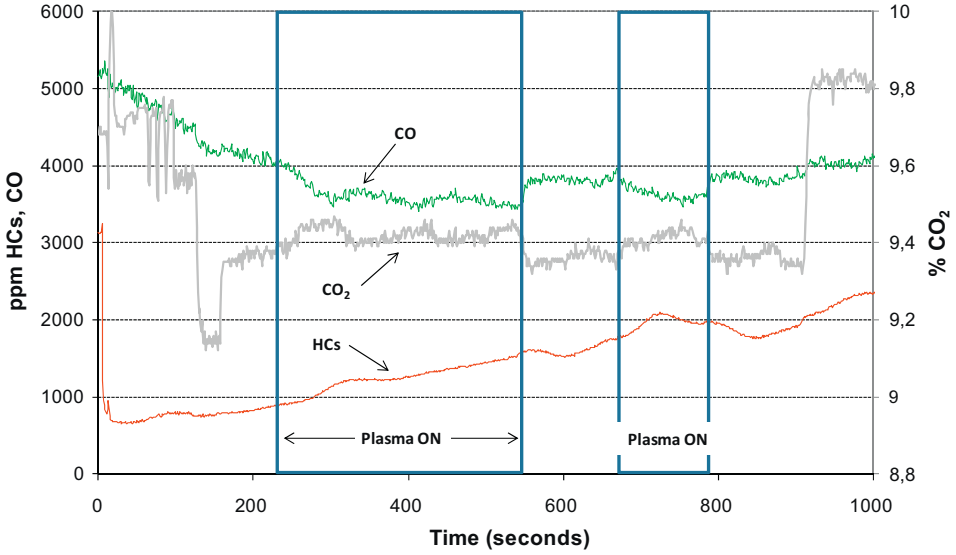

Fig. 8. Ozone injection experiment on exhaust from engine running at 1500 rpm, 2 bar. Ozone injection indicated by rectangles. Same experiment as shown in Fig. 5 but with CO and CO_2 data.

both measurement errors and uncertainty as to ozone reaction stoichiometry) with a calculation of heat generation that might be expected based on the exothermic reaction of ozone with carbon monoxide and unburned hydrocarbons.

Figs. 7 and 8 show the data for ozone injection at the 1500 rpm – 2 bar engine operating regime. Some instabilities in the CO_2 concentration are observed between 0 s and 200 s experiment time, but are unrelated to the injection of ozone. For this engine regime, the dynamics of HC storage caused greater variations in the outlet gas concentration of HCs because the total amount of HCs emitted by the engine was greater, causing a faster saturation of the storage material. The fact that emissions of both CO and HCs were higher for this operating point meant that, while the percentage reduction in CO was less than for the idle operating condition, the absolute amount of CO removed by ozone was considerably greater. As seen in Fig. 8, the change in CO_2 concentration when the ozone was turned off was about twice that for the idle condition, indicating that a greater amount of HCs were converted. The heat balance for this case gave a value in the range of 9–12 °C (depending again on ozone reaction stoichiometry), which is in very good agreement with the observed temperature increase in the range of 10–12 °C. Table 2 provides a summary of the data used for the heat balance calculation for the four different cases – for the ozone injection cases, two temperature increase values are given which are based on two different ozone reaction stoichiometries – one represented by reaction (3), and the other in which all three oxygen atoms react.

In summary, the injection of ozone appears in this investigation to be superior to the direct plasma treatment, however, this must be considered in light of the fact that pure oxygen was used for the generation of ozone. The advantages of ozone generation as compared to direct plasma are both in improved performance and in lower capital costs. The difference in operating costs as represented in the last two rows of Table 1 (energy density) would be negated or reversed if air was used for ozone generation in place of pure oxygen.

4. Conclusion

The use of non-thermal plasma to assist Diesel oxidation catalysis was investigated in two different modes of operation: in-line plasma and ozone injection, both upstream of the catalyst. The tests were done on the exhaust from an HCCI Diesel engine with high EGR rate operating in a steady state mode of operation and therefore light-off behavior was not investigated. The main contribution of the inline plasma was to give a thermal 'push' to the catalyst when it was near its light-off temperature, depending on what motor running condition was considered. It should be emphasized that more significant effects are to be expected in light-off conditions (not reachable in HCCI mode for the reported experiments).

The injection of ozone for the same conditions also resulted in additional heating of the catalyst, but purely because of the exothermic reaction of ozone with CO and adsorbed hydrocarbons, and gave a CO conversion of as much at 25%. While both techniques gave improvements in emissions, the ozone injection option might be more practical due to lower investment costs. This study only considers at the feasibility of ozone injection, the ozone generator being fed with pure oxygen. The efficiency of ozone production using dry air as feed gas would generally be about half the value found here, and a small increase in NO_x emissions will be introduced. Further investigations will be needed for the implementation of either option.

Acknowledgement

This work was supported by grants from the European Commission in the STREP PAGODE no. TST5-CT-2006-031404.

References

[1] T.V. Johnson, SAE Int. J. Fuels Lubr. 3 (2010) 16–29.
[2] M. Zheng, G.T. Reader, J.G. Hawley, Energy Convers. Manage. 45 (2004) 883–900.
[3] M.Y. Kim, C.S. Lee, Fuel 86 (2007) 2871–2880.
[4] B. Reveille, A. Kleemann, V. Knop, C. Habchi, Potential of Narrow Angle Direct Injection Diesel Engines for Clean Combustion: 3D CFD Analysis, SAE International, 2006, doi:10.4271/2006-01-1365.
[5] V. Knop, H. Kircher, S. Jay, P. Béard, A.P. da Cruz, O. Colin, Oil Gas Sci. Technol. – Revue De l'IFP 63 (2008) 21.
[6] B. Walter, P. Pacaud, B. Gatellier, Oil Gas Sci. Technol. – Revue De l'IFP 63 (2008) 18.
[7] K. Yoshida, T. Kuroki, M. Okubo, Thin Solid Films 518 (2009) 987–992.
[8] R.G. Tonkyn, S.E. Barlow, J.W. Hoard, Appl. Catal. B: Environ. 40 (2003) 207–217.
[9] K.G. Rappé, J.W. Hoard, C.L. Aardahl, P.W. Park, C.H.F. Peden, D.N. Tran, Catal. Today 89 (2004) 143–150.
[10] F. Holzer, U. Roland, F.-D. Kopinke, Appl. Catal. B: Environ. 38 (2002) 163–181.
[11] M. Okubo, N. Arita, T. Kuroki, K. Yoshida, T. Yamamoto, Plasma Chem. Plasma Process. 28 (2008) 173–187.
[12] M.J. Kirkpatrick, E. Odic, J.-P. Leininger, G. Blanchard, S. Rousseau, X. Glipa, Appl. Catal. B: Environ. 106 (2011) 160–166.
[13] U. Roland, F. Holzer, F.-D. Kopinke, Appl. Catal. B: Environ. 58 (2005) 217–226.
[14] U. Roland, F. Holzer, A. Pöppl, F.-D. Kopinke, Appl. Catal. B: Environ. 58 (2005) 227–234.
[15] M. Petersson, D. Jonsson, H. Persson, N. Cruise, B. Andersson, J. Catal. 238 (2006) 321–329.
[16] S. Calvo, S. Dupre, S. Eymerie, A. Goldman, M. Goldman, Y. Lendresse, System for Exhaust Gas Treatment Comprising a Gas Ionizing System with . . ., U.S. Patent 7,121,079 (2006).
[17] G.R. Chandler, A.F. Diwell, R.R. Rajaram, Combatting Air Pollution, U.S. Patent 6,546,717 (2003).
[18] B.K. Cho, J.-H. Lee, Method of Reducing NO_x in Diesel Engine Exhaust, U.S. Patent 7,090,811 (2006).
[19] H. Hirata, M. Kakinohana, M. Ibe, Exhaust Gas Purifying Apparatus and Method Thereof, U.S. Patent 7,299,624 (2007).
[20] E.D. Klomp, Air-assisted Fuel Injector with Ozone Enrichment, U.S. Patent 6,305,363 (2001).
[21] R.N. Miller, R.P. Caren, J.A. Ekchian, Method and Apparatus for Reducing Pollutants, U.S. Patent 5,806,305 (1998).
[22] A. Mfopara, M. Kirkpatrick, E. Odic, Plasma Chem. Plasma Process. 29 (2009) 91–102.